PHYSICAL REVIEW A **69**, 041604(R) (2004)

Echo spectroscopy of bulk Bogoliubov excitations in trapped Bose-Einstein condensates

E. Gershnabel, N. Katz, R. Ozeri, E. Rowen, J. Steinhauer,* and N. Davidson
Department of Physics of Complex Systems, Weizmann Institute of Science, Rehovot 76100, Israel
(Received 25 September 2003; published 23 April 2004)

We propose and demonstrate an echo method to reduce the inhomogeneous linewidth of Bogoliubov excitations, in a harmonically-trapped Bose-Einstein condensate. Our proposal includes the transfer of excitations with momentum $+q$ to $-q$ using a double two photon Bragg process, in which a substantial reduction of the inhomogeneous broadening is calculated. Furthermore, we predict an enhancement in the method's efficiency for low momentum due to many-body effects. As a proof of principle, the echo can also be implemented by using a four photon process, as is demonstrated experimentally.

DOI: 10.1103/PhysRevA.69.041604 PACS number(s): 03.75.Kk, 03.75.Lm, 32.80.−t

Bragg spectroscopy of a trapped Bose-Einstein condensate (BEC) has recently revealed many of the BEC's intriguing bulk properties such as global coherence [1], verification of the Bogoluibov excitation spectrum, superfluidity and the superfluid critical velocity, and suppression of low-momentum excitations due to quantum correlations of the ground state [2–4]. However, whereas the resonance frequency and the frequency integral of the dynamic structure factor $S(k,\omega)$ mainly reflect the bulk properties of the BEC, the frequency width of the spectrum is dominated by inhomogeneous broadening mechanisms [5]. The inhomogeneous broadening is due to Doppler broadening [1] and the inhomogeneous mean-field energy that is often well described within a local-density approximation (LDA). Even when the LDA picture is not complete, as in the recent observation of radial modes within the condensate, the inhomogeneous broadening (manifested as the envelope function of the multimode spectrum) still dominates [6,7]. Overcoming the inhomogeneous mechanisms (arising from the particular trap shape), opens the possibility of studying the homogeneous broadening mechanisms, that can reflect the intrinsic decoherence processes of the bulk excitations, e.g., elastic collisions with the BEC [8].

Here we propose an echo spectroscopic method, which reduces the inhomogeneous broadening of bulk Bogoliubov excitations in a BEC (in analogy to the familiar echo in two level atoms [9]). This method is based upon the transfer of Bogoliubov excitations from momentum $+q$ to $-q$, by a degenerate two-photon Bragg transition induced by an optical lattice, with wave number $2q$. Additional echo schemes for BEC have also been proposed [10], but they do not include an explicit momentum space reflection, as described above. Using the Gross-Pitaevskii equation (GPE), we calculate the line shape of the echo excitation spectrum and show a substantial reduction of the inhomogeneous broadening. We also show a surprising quantum enhancement of the efficiency of this method for low momentum, in contrast with the familiar suppression due to structure factor considerations [4]. Finally, we demonstrate the echo concept experimentally using an alternative scheme based on a four-photon Bragg transition. Such a scheme allows us to create $+q$ excitations by a two-photon Bragg process [2,3] and then transfer them to $-q$ excitations via a degenerate four-photon Bragg process, using the same laser beams. For our experimental parameters we show only a modest narrowing of the spectrum, and therefore these results should be viewed as a proof of principle experiment.

As shown in Fig. 1(b), a short two-photon Bragg pulse with wave number $+q$ initially excites the condensate uniformly [11], along the $\hat{z}$ axis of the cylindrically symmetric condensate. We then employ our echo scheme, shown schematically in Fig. 1(a). Specifically, the initial Bragg pulse is followed by a second, much longer Bragg pulse with wave number $2q$. For the frequency difference $\delta\omega \sim 0$ between the two Bragg beams, the echo resonance condition is fulfilled for a transition from the positive momentum q to the nega-

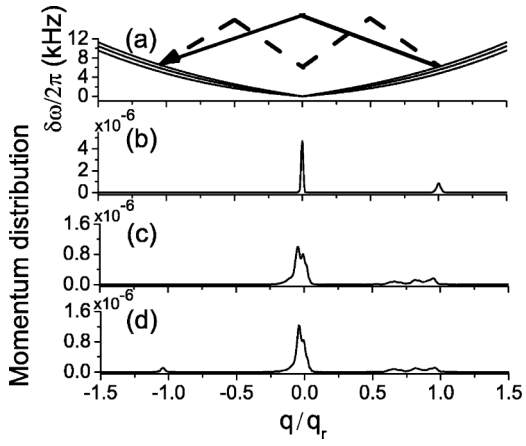

FIG. 1. The echo mechanism. (a) By application of the echo standing wave ($\delta\omega \approx 0$), $+q$ excitations are transferred to $-q$ excitations. The echo process can be achieved either by using a degenerate two-photon process (solid arrow) or a degenerate four-photon process (dashed arrow). (b)–(d) Cross sections of the wave function in longitudinal momentum space during the various echo steps, for a momentum $q_r = 8.06\ \mu\mathrm{m}^{-1}$, calculated with the GPE. The radial direction has been integrated. (b) After a 1.3 msec adiabatic Bragg pulse, (c) after the Bragg pulse and 4.2 msec delay. (d) As in (c), but with an adiabatic 4.2 msec two-photon echo pulse instead of the delay.

*Present address: Department of Physics, Technion–Israel Institute of Technology, Technion City, Haifa 32000, Israel.

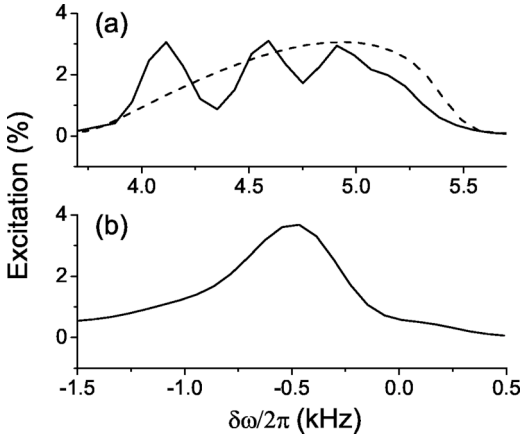

FIG. 2. Bragg and echo spectra for $q=8.06\ \mu\mathrm{m}^{-1}$ (free particle regime). (a) Excitation spectrum of the Bragg process calculated with an exact GPE simulation (solid line) and in the LDA (dashed line). (b) Excitation spectrum of the echo scheme from a GPE simulation.

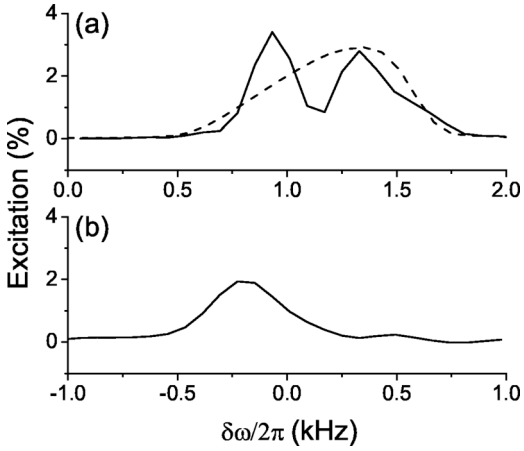

FIG. 3. Same GPE and LDA calculations as in Fig. 2, for the Bragg (a) and echo (b) spectra, only with $q=3.10\ \mu\mathrm{m}^{-1}$ (phonon regime). We observe narrowing of the echo spectrum. In a addition we note a smaller shift of the echo resonance, with respect to Fig. 2(b).

tive momentum $-q$, as indicated in Fig. 1(a) by the solid arrow and Fig. 1(d). The various dispersion curves in Fig. 1(a) are a schematic representation of the different local Bogoliubov dispersion relations due to the inhomogeneous local mean field. They can also represent different radial modes [6,7]. The echo line shape is expected to be free of inhomogeneous effects, as long as there are no transitions between the various curves, which belong to different positions within the condensate (essentially within the LDA) or different radial modes. Of course, the excitations do move along $\hat{z}$ during the process and therefore every curve is coupled with its vicinity, reflecting the fact that q is not a good quantum number in an inhomogeneous system of finite longitudinal size. This combination of inhomogeneous mean field and finite longitudinal size yields a residual small broadening of the spectrum. However, the strong broadening due to the radial dimension is overcome by the echo, leaving only the much narrower residual broadening in the axial dimension.

To verify the echo concept and calculate this residual broadening due to finite axial size, we use a simulation of the GPE [12] and calculate Bragg and echo processes for our experimental parameters [6]. Our experimental system contains $N=10^5$ atoms, confined in a harmonic trap with axial and radial angular frequencies $w_z=2\pi\times 26.5$ Hz and $w_r=2\pi\times 226$ Hz, respectively, chemical potential $\mu/h=2.06$ kHz, and LDA average healing length $\xi=0.23\ \mu$m. All excitations are axial, maintaining cylindrical symmetry [6].

Figure 1(b) shows the calculated momentum distribution after an initial 1.3 msec Bragg pulse, where the $q=0$ ground-state component and $+q$ excitations are seen. The Bragg excitation fraction is given as the integral of the wave function in momentum space, divided by $\hbar q$. Fig. 1(c) shows the calculated momentum distribution after an additional 4.2 msec of free evolution in the harmonic trap. The observed momentum components smaller than $+q$ are the fraction of the excitations which have left the condensate bulk during the free evolution and were consequently slowed by the external harmonic trap. Figure 2(d) shows the calculated momentum distribution after an initial 1.3 msec Bragg pulse and 4.2 msec echo pulse, where the appearance of a $-q$ momentum population is seen. The echo excitation fraction in Fig. 1(d) is obtained by subtracting its total momentum from the total momentum of Fig. 1(c), and then dividing by $2\hbar q$. To suppress nonlinear effects, we adiabatically increase and decrease the intensity of our pulses during the echo steps.

Using the GPE simulations, we first compare the spectrum of the Bragg and echo excitations in the high-momentum, free-particle regime shown in Fig. 2 for $q_r=8.06\ \mu\mathrm{m}^{-1}(q\xi=1.85)$. Figure 2(a) shows the calculated Bragg spectrum (using a 4.2 msec rectangular pulse). The multipeak structure, corresponding to the recently observed radial modes [6] is evident in the spectrum. The calculated full width at half maximum (FWHM) of the spectrum is 1.26 kHz. The dashed line in Fig. 2(a) is the LDA line shape [5]. Although lacking the multipeak structure, the LDA line shape has a very similar width to the exact GPE line shape [7]. Fourier broadening for a 4.2 msec rectangular Bragg pulse, Doppler broadening and the collisional broadening (not included in the GPE calculations) are 210.9, 135.5, and 35.1 Hz (FWHM), respectively, all much smaller than the inhomogeneous broadening [13].

Figure 2(b) shows the calculated echo spectrum. A narrow peak is seen close to $\delta\omega=0$, as expected. Comparison with Fig. 2(a) indicates that the echo has indeed reduced the inhomogeneous linewidth. Thus, the echo pulse does not mix the various radial modes. The echo FWHM is 0.59 kHz, 2.1 times smaller then the Bragg FWHM of Fig. 2(a). The Doppler broadening, however, is still not resolved. The observed $\sim$0.5 kHz negative shift of the resonance from $\delta\omega=0$ is probably due to the decrease in momentum of the outgoing excitations during the echo process (as explained above).

We repeat these calculations for low-momentum excitations in the phonon regime with $q=3.10\ \mu\mathrm{m}^{-1}$ $(q\xi=0.71)$. The resulting echo spectrum width [Fig. 3(b)] has a FWHM of 0.39 kHz, 1.7 times smaller than the FWHM of the Bragg spectrum shown in Fig. 3(a). The shift of the echo resonance

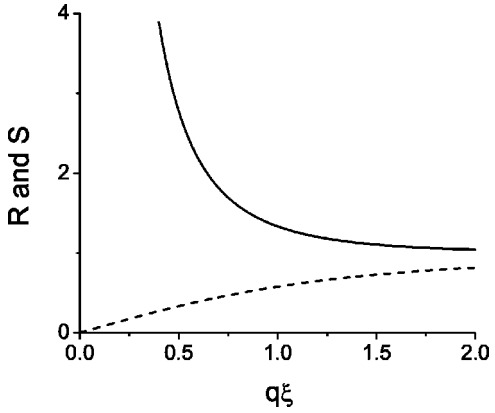

FIG. 4. The echo response R (solid line). The dashed line shows the structure factor S_q. Note the enhancement of R and the suppression of S_q for small q.

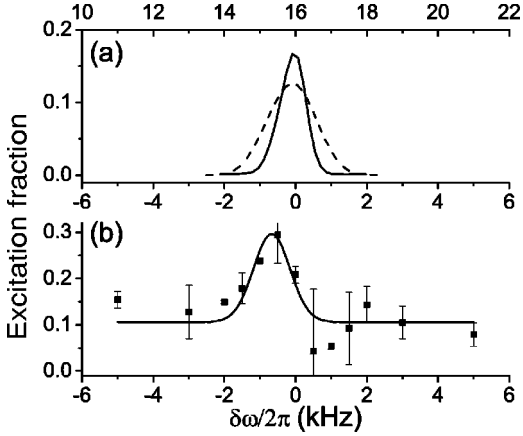

FIG. 5. (a) GPE predictions. The solid curve and the lower axis show the four-photon echo spectrum for the smoothly varying 1 msec pulse used in the experiment. The dashed curve and the upper axis correspond to the Bragg spectrum for the same pulse. (b) Experimental echo spectrum (squares) and a Gaussian fit (solid line).

from zero, seen in Fig. 3(b), is smaller than the high-momentum case of Fig. 2(b), as expected.

We verify numerically that the width of the echo spectrum increases for shorter and stronger echo pulses, indicating an increase of Fourier and power broadening. Thus, having chosen sufficiently weak and long pulses, the echo spectra of Figs. 2 and 3 are finite-size broadened. We also measure a decrease in the echo linewidth for longer condensates (having the same μ), in contrast to the Bragg process where the inhomogeneous linewidth is size independent. In fact, we expect the echo linewidth to approach the homogenous (collisional) linewidth for a long enough condensate having any finite μ.

Next, we calculate the echo transition rate in the approximation of an infinite, uniform Bogoliubov gas, and in analogy to the calculation of the Bragg rate [4]. The initial interaction Hamiltonian between the light and BEC is

$$\hat{H}' = C \sum_{klmn} \hat{c}_l^\dagger \hat{a}_n^\dagger \hat{c}_k \hat{a}_m \delta_{l+n-k-m}, \tag{1}$$

where C is the coupling constant, $\hat{c}(\hat{c}^\dagger)$ are the photonic annihilation (creation) operators and $\hat{a}(\hat{a}^\dagger)$ are the atomic annihilation (creation) operators. The first transition we analyze is that from $+q$ to $-q$, i.e., from the initial state $|i\rangle = |n_q, n_{-q}; N_q, N_{-q}\rangle$ to the final state $|f\rangle = |n_q+1, n_{-q}-1; N_q-1, N_{-q}+1\rangle$, where n_q represents the number of photons in the $+q$ direction and N_q represents the number of $+q$ Bogoliubov excitations. Since the excitations are axial, we refer only to the magnitudes of the momenta. In order to evaluate the transition matrix element, we must consider the matrix element of the Hamiltonian (1) between $|i\rangle$ and $|f\rangle$, and transform the atomic operators into Bogoliubov excitation operators. We find

$$\langle f|\hat{H}'|i\rangle_+ = C\sqrt{n_{-q}}\sqrt{n_q+1}\sqrt{N_q}\sqrt{N_{-q}+1}\{u_q^2+v_q^2\}, \tag{2}$$

where u_q and v_q are the Bogoliubov amplitudes [14] and the "+" notation represents the transition from $+q$ to $-q$. The second transition to be explored is the reverse process (transfer from $-q$ to $+q$), whose matrix element is denoted by $\langle f|\hat{H}'|i\rangle_-$. In the Fermi golden rule approximation the transition rate is given by $(2\pi/h)(|\langle f|\hat{H}'|i\rangle_+|^2 - |\langle f|\hat{H}'|i\rangle_-|^2)\delta(E_q - E_{-q})$. Assuming the initial condition $N_q \gg 1$, i.e., $(N_q+1) \approx N_q$, neglecting the $n_q N_{-q}$ term, and assuming a classical laser field (i.e., $n_q \gg N_{-q}$), the rate can be approximated by $(2\pi/\hbar)|C|^2 N_q n_{-q} n_q \{u_q^2+v_q^2\}^2 \delta(E_q - E_{-q})$. Hence, there is no Bosonic amplification due to the least populated mode (N_{-q} in our case). Considering the term $\{u_q^2+v_q^2\}^2$ and using the normalization $u_q^2 - v_q^2 = 1$ and the value of the structure factor $S_q = (u_q - v_q)^2$ we find that the echo rate per excitation with momentum q is proportional to the response R, defined by $R \equiv ((1+S_q^2)/2S_q)^2$. R has the low q asymptotic behavior of $(2S_q)^{-2}$, thus for low q (where S_q is small) we calculate a large enhancement in R.

The response is seen in Fig. 4 (solid line) to be greatly enhanced for small q, in contrast with the Bragg process, which is suppressed by the structure factor (dashed line). The existence of a significant negative momentum component in low-momentum Bogoliubov excitations gives rise to a strong amplification of the echo rate. This is in contrast with the destructive interference which occurs for regular Bragg pulses. We emphasize that the validity of these results is for the infinite homogeneous gas. We do not observe such an enhancement in the GPE calculations for a trapped BEC.

To demonstrate the echo spectroscopy experimentally, we use the apparatus described in Refs. [3], in which a nearly pure (>90%) BEC of 1×10^5 ^{87}Rb atoms in the $|F, m_f\rangle = |2,2\rangle$ ground state, is formed in a cylindrically symmetric magnetic trap. A two-photon Bragg transition and the subsequent four-photon echo transition are both induced by the same counter-propagating (along $\hat{z}$) laser beam pair, locked to a Fabry-Perot cavity line, detuned 44 GHz below the $5S_{1/2}, F=2 \rightarrow 5P_{3/2}, F'=3$ transition.

After exciting approximately 35% of the condensate by means of a short 0.1 msec rectangular Bragg pulse with $\delta\omega = 2\pi\times16$ kHz, we apply a 1 msec echo pulse with an envelope shaped as $\sin(\pi\times10^3 t)$ $(0<t<1$ msec), using the same

beams. We vary $\delta\omega$ to make a spectroscopic measurement of the echo response around $\delta\omega=0$, using the four-photon process to transfer excitations from $+q$ to $-q$ [Fig. 1(a), dashed arrow]. From the absorption images after 38 msec of time-of-flight we find the ratio between the $-q$ population N_{-q} and the total (not collided) amount of atoms $N_q+N_{BEC}+N_{-q}$. The measured echo spectrum is shown in Fig. 5(b) together with a Gaussian fit to the data, centered close to zero frequency, and with a FWHM of 1.21 kHz. The experimental echo duration is limited by collisions, which are not taken into account in our GPE simulation and cause a significant degradation in our signal for echo times longer than 1 msec. Sloshing of the condensate [6] may also cause a broadening of the measured spectrum width. However, we still observe a sub-Fourier broadening of the echo spectrum, which is also predicted by a GPE simulation (for four-photon echo), as shown by the solid line in Fig. 5(a) (FWHM 0.86 kHz). The dashed line in Fig. 5(a), corresponds to a standard Bragg spectrum [1–3,6] of a 1 msec pulse (with the same envelope as the echo), and is Fourier limited (FWHM 1.63 kHz). The sub-Fourier width of the echo spectrum is possible due to the nonlinearity of the four-photon process. Thus, with relatively short pulses, a narrowing of the lineshape is achieved, as compared to standard Bragg spectroscopy [2,3].

In conclusion, we implement a spectroscopic echo method in momentum space in order to reduce the measured inhomogeneous linewidth of Bogoliubov excitations in a trapped BEC. We note that by varying the shape of the trap (either in length or in functional form) the collisional and finite-size broadenings may be reduced further than reported here. We also predict an enhancement of the echo rate at low momentum emerging from constructive interference of the amplitudes of various quantum paths for this process. This is in contrast to the usual suppression of low momentum processes in quantum degenerate Boson systems.

This work was supported in part by the Israel Ministry of Science and the Israel Science Foundation.

[1] J. Stenger, S. Inouye, A. P. Chikkatur, D. M. Stamper-Kurn, D. E. Pritchard, and W. Ketterle, Phys. Rev. Lett. **82**, 4569 (1999); **84**, 2283 (2000).

[2] D. M. Stamper-Kurn, A. P. Chikkatur, A. Görlitz, S. Inouye, S. Gupta, D. E. Pritchard, and W. Ketterle, Phys. Rev. Lett. **83**, 2876 (1999).

[3] J. Steinhauer, R. Ozeri, N. Katz, and N. Davidson, Phys. Rev. Lett. **88**, 120407 (2002).

[4] W. Ketterle and S. Inouye C. R. Acad. Sci., Ser IV: Phys., Astrophys. **2**, 339 (2001).

[5] A. Brunello, F. Dalfovo, L. Pitaevskii, S. Stringari, and F. Zambelli, Phys. Rev. A **64**, 063614 (2001).

[6] J. Steinhauer, N. Katz, R. Ozeri, N. Davidson, C. Tozzo, and F. Dalfovo, Phys. Rev. Lett. **90**, 060404 (2003).

[7] C. Tozzo and F. Dalfovo, New J. Phys. **5**, 54 (2003).

[8] N. Katz, J. Steinhauer, R. Ozeri, and N. Davidson, Phys. Rev. Lett. **89**, 220401 (2002).

[9] L. Allen, J. H. Eberly, *Optical Resonance and Two-Level Atoms* (Dover, New York, 1987).

[10] A. B. Kuklov and N. Chencinski, Phys. Rev. A **57**, 4699 (1998).

[11] The Bragg pulse must be short enough such that its Fourier broadening dominates any other broadening mechanism to excite the condensate uniformly.

[12] We numerically solve the GPE $i\hbar\partial_t\psi=\{-\hbar^2\nabla^2/(2m)+V+g|\psi|^2\}\psi$, with $V(\vec{r},t)=m/2(w_r^2r^2+w_z^2z^2)+\Omega(t)V_B\cos(qz-\delta\omega t)$. g is the mean-field coupling constant, m is the ^{87}Rb atomic mass, q is the wave number of the excitation, V_B is the potential intensity and $\Omega(t)$ is an envelope function. Using cylindrical symmetry we evolve ψ on a two-dimensional grid N_zN_r (up to 4096×32), using the Crank-Nicholson differencing method.

[13] The Doppler line shape prediction is $|\psi(p_z)|^2\sim\{2(4+\kappa^2)J_1(\kappa)J_2(\kappa)+\kappa J_0(\kappa)[5\kappa J_1(\kappa)-16J_2(\kappa)+3\kappa J_3(\kappa)]\}/\kappa^3$ [1], where $\kappa\equiv p_zz_0/\hbar$, z_0 and p_z are the axial Thomas-Fermi radius and the initial condensate momentum, respectively. We take $\hbar\omega-\hbar\omega_0=p_z\cdot\hbar q/m$ where $\hbar q$ is the momentum given to the condensate and $\hbar\omega_0$ is the free particle resonance energy. The collisional line shape is approximated by the Lorenzian $1/[(\omega-\omega_0)^2/(2\pi)^2+(\Gamma/2)^2]$ where $2\pi\Gamma$ is the collision rate [8].

[14] A. Fetter, in *Bose-Einstein Condensation in Atomic Gases*, Proceedings of the International School of Physics "Enrico Fermi," Course CXL, edited by M. Inguscio, S. Stringari, and C. Wieman (IOS Press, Amsterdam, 1999).